equivalent to 0.01 mm year^{-1} of eustatic sea level rise. If the entire grounded section of PIG were lost to the ocean, we estimate the net contribution to eustatic sea level to be 6 mm (*18*). Both of these are small in comparison with other expected changes in sea level (*1*). On the other hand, if sufficiently prolonged, the present thinning could affect the flow of what is now slow-moving ice in the interior, increasing the volume of rapidly drained ice (*10*).

References and Notes

1. R. Warrick, C. Le Provost, M. Meier, J. Oerlemans, P. Woodworth, in *Climate Change 1995: The Science of Climate Change* (Cambridge Univ. Press, Cambridge, 1966), pp. 359–405.
2. C. R. Bentley, M. B. Giovinetto, in *Proceedings of the International Conference on the Role of Polar Regions in Global Change* (Univ. of Alaska, Fairbanks, AK, 1991), pp. 481–488. The authors obtained 26 Gt year^{-1} for the ice discharge flux of PIG. We used the improved estimate of 75 Gt year^{-1} determined by Rignot *et al.* (*24*).
3. J. Weertman, *J. Glaciol.* **13**, 3 (1974).
4. R. H. Thomas, *J. Glaciol.* **24**, 167 (1979).
5. V. Barcillon, D. R. Macayeal, *J. Glaciol.* **39**, 131 (1993).
6. C. J. Van der Veen, *Quat. Res.* **24**, 257 (1985).
7. R. C. H. Hindmarsh , *Ann. Glaciol.* **23**, 105 (1996).
8. J. H. Mercer, *Nature* **271**, 321 (1978).
9. T. J. Hughes, *J. Glaciol.* **27**, 518 (1981).
10. D. Lindstrom, T. J. Hughes, *Antarct. J. U.S.* **19**, 56 (1984).
11. M. Oppenheimer, *Nature* **393**, 325 (1998).
12. E. J. Rignot, *Science* **281**, 549 (1998).
13. We followed the method described (*16*) in forming time series at crossovers of the orbit ground tracks. We examined trends in the backscattered power throughout the basin. We detected no significant correlation at any scale and applied no empirical correction (*16*) for variation in the ratio of surface-to-volume scattering. Because the crossover locations do vary in detail with time, the elevations were corrected for surface slope (*25*) with an interferometrically derived elevation model of the basin. The surface slope was less than 1.1° ± 0.1° all over and the mean relocation distance for altimeter footprints was 1.2 ± 0.1 km (~12.5% of the footprint diameter). The associated height correction does not affect calculations of elevation change. The variability of the elevation time series linear trends was ~0.3 m year^{-1}, due in part to measurement error and in part to accumulation fluctuations (*16*).
14. M. D. Stenoein, C. R. Bentley, *J. Geophys. Res.* **105**, 21761 (2000).
15. We differenced pairs of ERS repeat pass interferograms to determine the ice surface speed in the look direction of the SAR (*26–28*). When pairs of interferograms were not available, the topographic signal was separated from the velocity signal with a coarse resolution digital elevation model. The surface velocity vector was calculated with measurements of speed in independent look directions (*28*). We mapped 26% (~42,000 km^2) of the PIG drainage basin, or 48% of the region north of 76.5°S (which includes the vast majority of the glacier and tributary network), using a combination of ascending and descending (49 and 32% of the basin, respectively) SAR scenes. To obtain the interferometer baseline, we combined ice sheet balance velocities (*29*) for the slow-moving interior, feature-tracked velocities close to the grounding line, and surface elevation tie-points (*30*). The principal error in the velocity arose from the inadequate distribution of control points. The SD of velocity differences between overlapping images forming the mosaic was ~60 m year^{-1}. (Long wavelength errors may also be present but are not relevant to the work described here).
16. D. J. Wingham, A. J. Ridout, R. Scharroo, R. J. Arthern, C. K. Shum, *Science* **282**, 456 (1998).
17. D. G. Vaughan *et al.*, *Antarct. Res. Ser.* **77**, 236 (2001).
18. The areal extent of the fast-flowing glacier is ~5300 km^2, or ~3% of the drainage basin. From the data in Fig. 4A, we estimate the volume of ice overburden to be ~2100 km^3 of ice (that is, ~6 mm of eustatic sea level). At an average rate of thinning (Fig. 3) of 0.75 m year^{-1}, this volume will be removed in 527 years.
19. Katabatic winds are gravity-driven air flows (*31*). We estimated the interannual variability of wind speed and air temperature from coarse resolution reanalysis fields. We estimated the variability of the annual sublimation rate of PIG to be 0.13 m year^{-1} water equivalent using the empirical equation of Bintanja (*32*). We also estimated the variability in erosion due to drifting snow, using the formula of Budd (*33*), and this was negligible. Although old samples collected from locations close to the grounding line of PIG (*34*) indicate that the surface density may be closer to that of ice (917 kg m^{-3}) than snow (350 kg m^{-3}), assuming a value of 400 kg m^{-3} provides an interannual variability of elevation of 0.32 m year^{-1}. Assuming that the variability is independent from year to year, the 7-year variability of thickness due to ablation is 0.12 m year^{-1}.
20. A. J. Payne, *J. Geophys. Res.* **100**, 4249 (1995).
21. T. B. Kellogg, D. E. Kellogg, *J. Geophys. Res.* **92**, 8859 (1987).
22. R. B. Alley, I. M. Whillans, *J. Geophys. Res.* **89**, 6487 (1984).
23. A. C. Fowler, E. Shiavi, *J. Glaciol.* **14**, 104 (1998).
24. E. Rignot, D. G. Vaughan, M. Schmeltz, T. K. Dupont, D. R. Macayeal, in preparation.
25. J. Bamber, *Int. J. Remote Sens.* **15**, 925 (1994).
26. R. M. Goldstein, H. Engelhardt, B. Kamb, R. M. Frolich, *Science* **262**, 1525 (1993).
27. R. Kwok, M. A. Fahnestock, *IEEE Trans. Geosci. Remote Sens.* **34**, 1 (1996).
28. I. Joughin, R. Kwok, M. Fahnestock, *IEEE Trans. Geosci. Remote Sens.* **36**, 25 (1998).
29. W. F. Budd, R. C. Warner, *Ann. Glaciol.* **23**, 21 (1996).
30. H. A. Zebker, R. M. Goldstein, *J. Geophys. Res.* **91**, 4993 (1986).
31. T. R. Parish, D. H. Bromwich, *Nature* **328**, 51 (1987).
32. R. Bintanja, *Ann. Glaciol.* **27**, 251 (1998).
33. M. R. van den Broeke, R. Bintanja, *J. Glaciol.* **41**, 395 (1995).
34. T. B. Kellogg, D. E. Kellogg, T. J. Hughes, *Antarct. J. U.S.* **20**, 79 (1985).

35. Supported by the UK Natural Environment Research Council. Feature-tracked ice speed data were provided by the Earth Observing System Distributed Active Archive Center at the National Snow and Ice Data Center, University of Colorado, Boulder, CO. Wind speed data were provided by the National Center for Atmospheric Research, Boulder, CO.

14 September 2000; accepted 2 January 2001

Scale Dependence in Plant Biodiversity

M. J. Crawley* and J. E. Harral

The relationship between the number of species and the area sampled is one of the oldest and best-documented patterns in community ecology. Several theoretical models and field data from a wide range of plant and animal taxa suggest that the slope, z, of a graph of the logarithm of species richness against the logarithm of area is roughly constant, with $z \approx 0.25$. We collected replicated and randomized plant data at 11 spatial scales from 0.01 to 10^8 square meters in Great Britain which show that the slope of the log-log plot is not constant, but varies systematically with spatial scale, and from habitat to habitat at the same spatial scale. Values of z were low (0.1 to 0.2) at small scales (<100 square meters), high (0.4 to 0.5) at intermediate scales (1 hectare to 10 square kilometers), and low again (0.1 to 0.2) for the largest scale transitions (e.g., East Berks to all of Berkshire). Instead of one process determining changes in species richness across a wide range of scales, different processes might determine plant biodiversity at different spatial scales.

Understanding the determinants of species richness is central to many questions in both pure and applied ecology. At the largest spatial scales and over the longest time scales, species richness is determined by rates of speciation and extinction (*1*). At smaller spatial scales and over shorter periods of time, the number of species is determined by the birth, death, and dispersal rates of individuals interacting with populations of competitors, mutualists, and natural enemies (*2*). In all cases, however, the number of species depends on the area sampled (*3–5*), the absolute abundances of the species (*4*, *6*, *7*), their spatial patterns (*8*, *9*), and the degree of mixing of species (*10*, *11*). The relationship between species richness and area is particularly important in biodiversity studies because it holds out the prospect of predicting species richness at large scales from data gathered relatively inexpensively at much smaller scales (*12*, *13*). It is conventional to use the power law $S = cA^z$ to describe the relationship between species richness S and the area sampled A. The exponent, z, is close to 0.25 for several theoretical models (*14–16*) and for much field data (*1*), but there are also data where z is greater than 0.25 [e.g., on islands, and at large scales generally (*1*)], and data where the slope is less than 0.25 [e.g., with smaller, plant-sized quadrats (*17–19*)].

Two fundamentally different processes

Department of Biology, Natural Environment Research Council Centre for Population Biology, Imperial College, Silwood Park, Ascot SL5 7PY, UK.

*To whom correspondence should be addressed. E-mail: m.crawley@ic.ac.uk

Table 1. Vascular plant species richness in Silwood Park at scales from 0.01 m^2 to 110 ha. *S*, species richness; Var *S*, variance in species richness; CV *S*, coefficient of variation in species richness (standard deviation divided by the mean); Min *S*, minimum; Med *S*, median; Max *S*, maximum species richness; *z*, slope of the log(Species)/log(Area) transition from this scale to the scale immediately above; *n*, replication at this scale; SE(*z*) = standard error of the slope; Cl 0.025, lower 2.5 percentile of the simulated distribution of *z* based on 1000 randomizations; Cl 0.975, upper 97.5 percentile of *z*; *m*, replication for the simulations (half of the smaller of the two adjacent *n* values). NA, not applicable.

	0.01 m^2	0.1 m^2	1 m^2	10 m^2	100 m^2	1000 m^2	1 ha	4 ha	9 ha	16 ha	25 ha	110 ha
Mean *S*	3.06	4.78	6.38	9.99	16.23	34.88	81.90	164.6	257.6	338.5	417.3	686
Var *S*	2.35	6.40	15.00	31.79	112.19	317.2	1212.4	1949.8	2166.9	3433.7	7480.3	NA
CV *S*	0.50	0.53	0.61	0.56	0.63	0.51	0.42	0.27	0.18	0.17	0.21	NA
Min *S*	1	1	1	1	1	7	28	87	208	274	362	NA
Med *S*	3	5	6	10	16	32	72	154	253	332	373	NA
Max *S*	7	13	19	28	47	90	209	239	345	416	517	NA
z	0.18	0.10	0.20	0.20	0.37	0.39	0.53	0.57	0.48	0.46	0.37	NA
n	346	345	259	239	88	67	110	18	7	4	3	1
SE (*z*)	0.017	0.015	0.014	0.014	0.014	0.010	0.015	0.037	0.062	0.087	0.001	NA
Cl 0.025	0.158	0.077	0.152	0.132	0.234	0.296	0.294	0.241	NA	NA	NA	NA
Cl 0.975	0.228	0.173	0.246	0.307	0.417	0.449	0.709	0.890	NA	NA	NA	NA
m	170	125	115	44	33	33	9	4	NA	NA	NA	NA

anchor the opposite ends of a species-area curve. The lower end is essentially a packing problem: The number of species in a small area depends on the size of the individuals and on the extent to which they are vertically stratified or horizontally intermingled with each other. The upper end is a species-pool problem: How many species are there in the local biota from which the current sample might reasonably be expected to be drawn? There are several reasons why species accumulate as the sample area is increased: Less abundant species are recorded as a larger total number of individual plants is included (a sampling effect); spatially aggregated species are encountered that were missed at first (a spatial clumping effect); species that are ecologically separated within the same habitat will occur together only in larger quadrats (a spatial segregation effect); and distinctive new sets of species are added as different plant communities are included (a habitat effect). The apparent constancy of the slope of the species-area relation suggests that there might be a single (probably simple) mechanism that integrates the effects of all these different processes on species richness (*14*, *15*, *20–23*). A simple calculation, however, shows that a power law relation between species richness and area with slope $z = 0.25$ could not be global. We know that there are 250,000 species of vascular plants on Earth (*24*), and that the land surface is 1.4×10^8 km^2. The power law predicts that $c = S/A^z = 250{,}000/(1.4 \times 10^8 \times 10^6)^{0.25} = 72.7$ species at a scale of 1 m^2. This is off by an order of magnitude. If *z* is not a constant (*1*, *12*, *19*), then we can ask whether the slope of the species-area relationship shows characteristic scale dependence, or whether variation in *z* is entirely idiosyncratic.

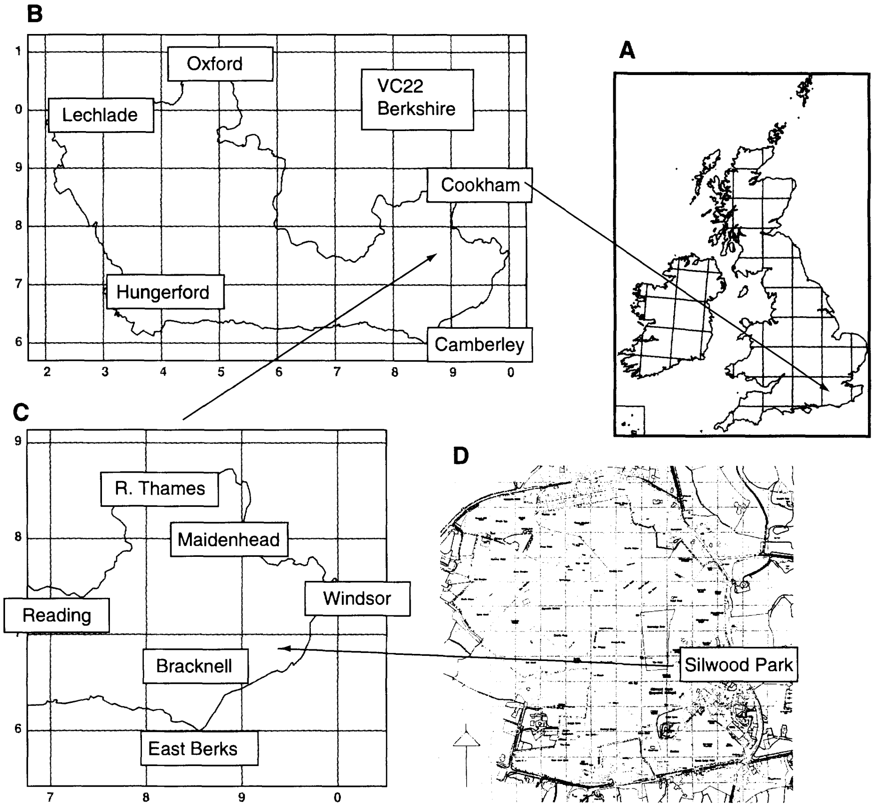

Fig. 1. (**A** to **D**) The study area was the Watsonian vice-county of Berkshire (VC22), a land-locked area west of London, that comprises the modern county of Berkshire plus the part of modern Oxfordshire that lies south of the River Thames. East Berkshire is the part of VC22 that lies east of Reading (east of OS Grid Line SU 700600). Silwood Park is an estate of 110 ha south of Windsor and east of Bracknell (centered on SU 940690); map (D) shows the grid lines used to define the boundaries of the 1-ha scale survey within Silwood Park. The grid scales are 100 km (A), 10 km [(B) and (C)], and 100 m (D).

We studied the flora of the county of Berkshire in southeast England (*25*, *26*). The whole county (1876 km^2) was sampled as a nested set of contiguous quadrats at 100 and 25 km^2 (Fig. 1). We surveyed 456 contiguous 1-km^2 quadrats in East Berkshire. Within Silwood Park, in the eastern part of East Berkshire, we studied all of the 110 contiguous 1-ha plots that make up the estate and its immediate neighborhood. At smaller scales, we took random samples within Silwood Park from quadrats of 1000, 100, 10, 1, 0.1, and 0.01 m^2. All vascular plant species, native and alien, were counted (*27*), except those that were obviously planted. The flora of towns, villages, and industrial waste ground was treated in exactly the same way as the flora of nature reserves, ancient woodlands, and other fragments of seminatural vegetation.

The species-area relationships are shown in Fig. 2. The analyses of the Silwood Park (Fig. 2A) and Berkshire (Fig. 2B) data were carried out separately to ensure that the higher recording effort within Silwood Park was not confounded with any differences in the shape of the species-area relationship (Tables 1 to 3). If the replication is averaged away, both graphs conform closely to the classical species-area model (dotted lines in Fig. 2); regressions of log(mean species richness) against log(area) gave slopes of 0.302 (SE = 0.019) for Silwood (Fig. 2A) and 0.267 (SE = 0.020) for Berkshire and Great Britain (Fig. 2B). These are not significantly differ-

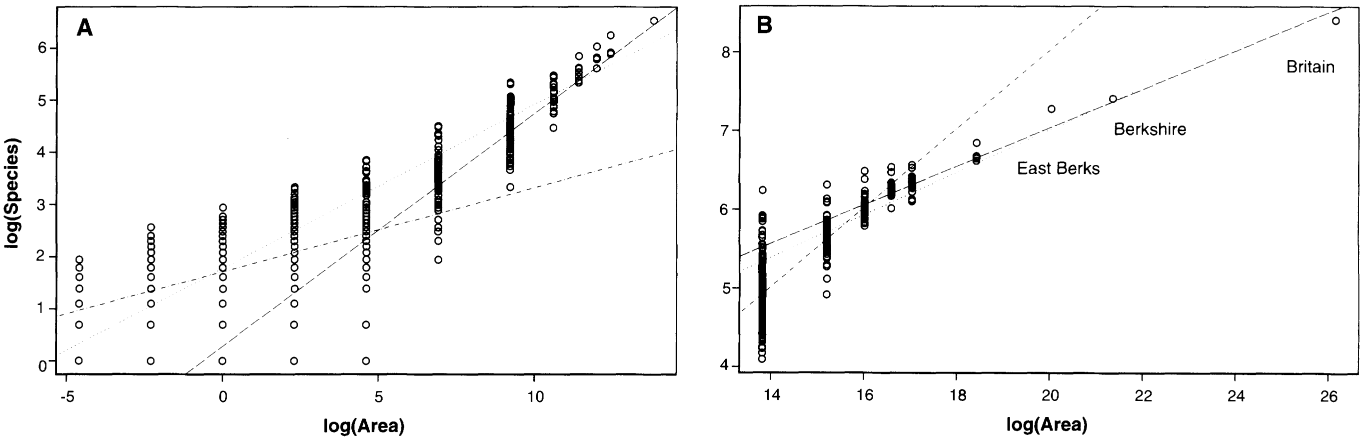

Fig. 2. (**A**) Vascular plant species richness in Silwood Park at scales from 0.01 m^2 to 110 ha. The smaller quadrats (up to 1000 m^2) were located at random within habitats, whereas data from the contiguous 1-ha plots were aggregated to obtain species richness at larger scales. Piecewise linear regression highlights the strength of the scale dependence in slope: The small-scale data (less than 1000 m^2) have a slope of $z = 0.161$ (SE = 0.0066, df = 1275; dashed and dotted line), whereas the larger scale data (1000 m^2 upward) have a much steeper slope of $z = 0.447$ (SE = 0.0204, df = 208; dashed line). (**B**) Vascular plant species richness at a range of spatial scales in East Berkshire (465 km^2), Berkshire as a whole (1876 km^2), and Great Britain (2.299 × 10^5 km^2). For East Berkshire, the data were aggregated from contiguous samples of 1 km^2 to scales of 4, 9, 16, and 25 km^2. For West Berkshire the data were accumulated from 25-km^2 samples gathered as part of the Atlas 2000 project of the Botanical Society of the British Isles. The data for Great Britain come from Stace (*27*). Piecewise linear regression again highlights the strength of the scale dependence in slope: data from intermediate scales (1 to 16 km^2) have a slope of $z = 0.502$ (SE = 0.014, df = 617; dashed and dotted line), whereas data from the largest scales (25 km^2 upward) have a much shallower slope of $z = 0.2448$ (SE = 0.012, df = 31; dashed line). Dotted lines denote the classical species-area model.

Table 2. Vascular plant species richness at a range of spatial scales in East Berkshire (465 km^2), Berkshire as a whole (1876 km^2), and Great Britain (2.299 × 105 km^2). Abbreviations as in Table 1.

	1 km^2	4 km^2	9 km^2	16 km^2	25 km^2	100 km^2	East Berks 465 km^2	All Berks 1876 km^2	Great Britain 2.299 × 10^5 km^2
Mean *S*	144.5	292.3	417.9	523.3	545.4	801.7	1448	1654	4500
Var *S*	2410.2	3580.8	4037.3	3215.3	4756.6	3911.9	NA	NA	NA
CV *S*	0.34	0.20	0.15	0.11	0.13	0.08	NA	NA	NA
Min *S*	60	137	327	409	448	749	NA	NA	NA
Med *S*	140	292	410	512	545	786	NA	NA	NA
Max *S*	512	552	655	689	709	939	NA	NA	NA
z	0.530	0.453	0.399	0.088	0.281	0.369	0.101	0.208	NA
n	465	91	40	23	23	7	1	1	1
SE (*z*)	0.025	0.043	0.058	0.076	0.036	0.049	NA	NA	NA
CI 0.025	0.432	0.337	0.228	−0.068	0.205	NA	NA	NA	NA
CI 0.975	0.583	0.545	0.541	0.248	0.353	NA	NA	NA	NA
m	45	20	11	11	4	NA	NA	NA	NA

Table 3. Species retention and variability at different scales within Silwood Park. Retention, defined here as the fraction of species found at scale $i + l$ that is present at scale *i*, shows no clear overall trend with scale, but mean retention is somewhat higher for the four smallest scales (0.66) than for the next four powers of 10 in scale (0.48). Relative variability [RV, measured as the standard deviation in log(Species) at a given scale] shows a pronounced peak in 100-m quadrats (as does the CV in Table 1). This suggests that quadrats larger than 100 m^2 (e.g., 33.3 m by 33.3 m or 50 m by 20 m) ought to be used when the intention is to characterize the α diversity of habitats by ensuring the inclusion of as full a set as possible of species that are faithful to the community in question. This result suggests that the quadrats used in the National Vegetation Classification (*31*) were too small to give robust estimates of fidelity [1000-m^2 quadrats (*32*) would have been preferable to the 4- and 100-m^2 quadrats used in grassland and woodland, respectively].

	Area (m^2)										
	0.01	0.1	1	10	100	1000	10^4	10^6	4 × 10^6	25 × 10^6	100 × 10^6
Retention	0.6	0.83	0.6	0.625	0.5	0.444	0.511	0.483	0.695	0.482	NA
RV	0.57	0.65	0.73	0.75	0.82	0.56	0.40	0.30	0.20	0.27	0.17

ent from one another nor from $z = 0.25$ (SE difference = 0.0348, $P = 0.32$). However, when the replication at each scale is used (in a log-linear model corrected for overdispersion), we find highly significant differences in slope from scale to scale (*28*); the same conclusion is reached by simulation (*29*). A visual impression of the nonconstancy of slope is obtained by piecewise regression. For both Fig. 2, A and B, extrapolation of a regression based on the left-hand half of the data is a very poor predictor of the right-hand half of the data (and vice versa).

Variation in slope with scale is summarized in Fig. 3. Slopes of the species-area relation were shallower at small scales where ecological interactions between individual plants were most important (e.g., competition or limited seed dispersal) and steeper at intermediate scales where geology, topography, hydrology, and management create a matrix of habitats that have more or less distinct floras. At the largest spatial scales, the slopes were shallow, reflecting the relatively low species turnover with distance that is characteristic of temperate forest biomes [in contrast, say, to the Cape Province of South Africa, where species turnover with distance is exceptionally high (*24*)].

There were also significant differences in the species-area relationships of different habitats. Figure 4A compares the species-area curves of grassland and woodland (the two most widespread habitats in Silwood Park). Grassland was more species-rich than woodland at all scales, but woodland showed much more pronounced scale-dependent changes in slope (Tables 4 and 5). Figure 4B compares built and waste ground (the most species-rich habitat in Silwood Park) with bracken (the most species-poor). These habitat differences in z reflect differences in plant size (large in woodlands, small in grassland) and life history (annuals and biennials in built habitats, long-lived perennials in grassland). Small-scale species richness is greatest when total population density is highest (individual plants are small) and sites are not preempted for long periods by the same individuals (turnover is rapid).

For all but the smallest quadrats, the variance in species richness was much greater than the mean (Tables 1 and 2). For example, the most species-rich 0.1 m by 0.1 m quadrat contained the same number of species ($S = 7$) as the most species-poor 33.3 m by 33.3 m quadrat (five orders of magnitude larger). A power-law regression of the logarithm of variance in species count against the logarithm of mean species count has a slope of 1.578 (SE = 0.23, $r^2 = 0.98$), reflecting the extremely high spatial aggregation of species richness ["hot spots" (*11*)]. The inclusion of major new plant communities (e.g., coastlands and uplands) accounts for the relatively steep transition from Berkshire to Great Britain ($z = 0.21$) compared with the relatively shallow transition from East Berks to all of Berkshire ($z = 0.10$) (Fig. 2B).

This analysis shows a clear pattern in the way that the slope of the species-area relationship changes with scale (Fig. 3). For the small scales over which individual plants interact (square centimeter to square meter), z is small ($0.1 < z < 0.2$) but strongly habitat-dependent (Fig. 4). The most rapid changes in species richness ($0.4 < z < 0.6$) occur at

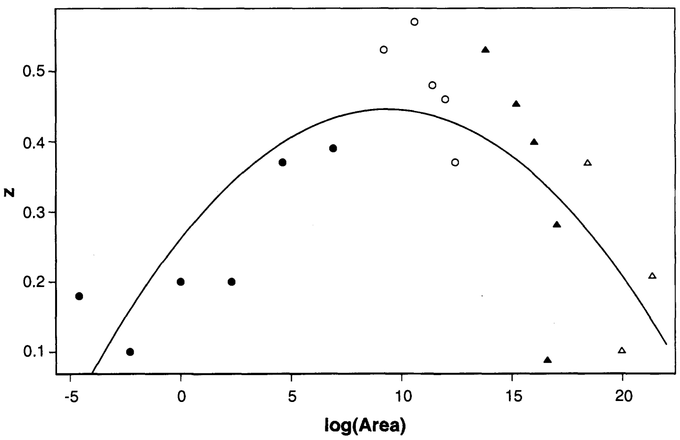

Fig. 3. Scale dependence in the slope of the species-area relationship. The slope of the log species–log area curve, z, plotted against the smaller of the two log-areas from which the slope was calculated. The slope shows a pronounced peak at intermediate scales (1 ha to 4 km^2), with low values for small quadrats (0.01 to 10 m^2) and at the landscape level (more than 10 km^2). The fitted line shows z as a function of log(Area): $z = 0.264 + 0.0396\ \log(\text{Area}) - 0.0021\ \log(\text{Area})^2$; the quadratic term (SE = 0.0005, df = 16) demonstrates the significance of the hump in the relation ($P = 0.0004$). The data are of four kinds, differing in the way they were collected and hence in the likelihood of underrecording. (●) Random samples within Silwood Park from 0.01 to 1000 m^2; (○) nested samples within Silwood Park from 1 to 110 ha; (▲) nested samples within East Berkshire from 1 to 100 km^2; (△) large-scale transitions above 100 km^2. The risk of underrecording increases with sample area for the random quadrats, because each quadrat is visited only once. The risk of underrecording declines with sample area for the nested quadrats, because each count is based on a progressively larger number of independent visits.

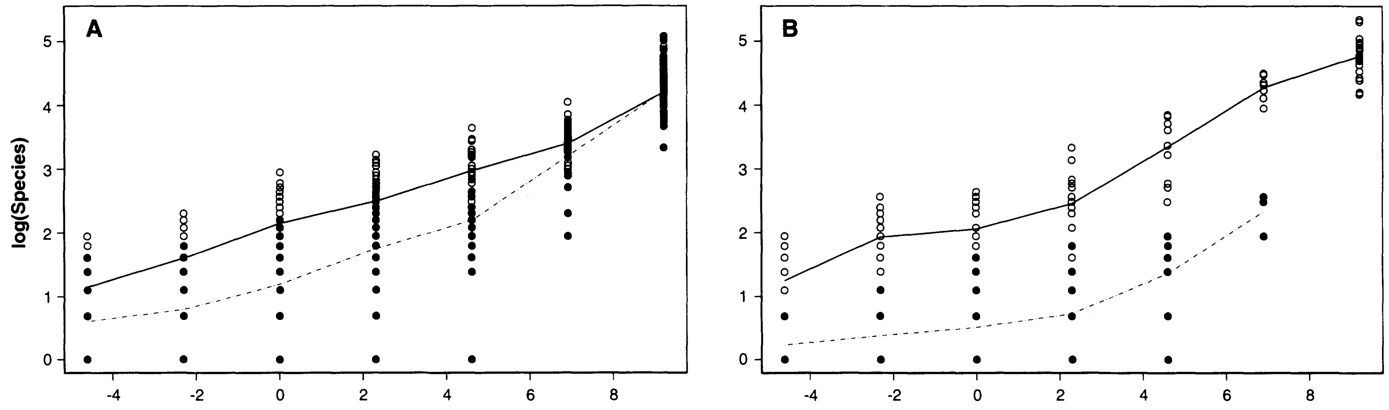

Fig. 4. Habitat differences in species-area curves within Silwood Park. (**A**) Comparision of grassland (open symbols; upper, solid line) with woodland (solid symbols; lower, dashed line). (**B**) Comparison of built and waste ground (open symbols; upper, solid line) with bracken (solid symbols; lower, dashed line). Mean species richness differed significantly between habitats at the same scale (log-linear model with Poisson errors corrected for overdispersion; $F = 184.05$, df = 5, 1447, $P < 0.000001$). The slopes of the scale-to-scale transitions differed between habitats at the same scale, and from scale to scale within the same habitat [habitat by log(Area) interaction deviance = 268.26; $F = 7.13$, df = 5, 1442, $P < 0.000001$]. The z values (slopes) for each scale transition in each habitat are shown in Table 5.

Table 4. Habitat differences in species richness within Silwood Park. Mean species richness in six habitats sampled at seven spatial scales from 0.01 to 10,000 m^2.

Habitat	Area (m^2)						
	0.01	0.1	1	10	100	1,000	10,000
Grassland	3.5	5.3	9.3	13.4	20.3	31.7	70.5
Woodland	2.0	2.5	3.8	6.8	10.5	27.1	71.5
Built	3.7	7.2	8.4	12.7	31.1	73.3	123.2
Bracken	1.3	1.6	2.0	2.5	4.4	10.7	n.a.
Heath	1.4	2.0	3.1	5.3	11.5	49.0	65
Fallow	4.4	7.4	10.3	14.3	24.1	40.7	83.7

Table 5. The slopes, z, of the scale-to-scale transitions within each of the habitats in Silwood Park. None of the bracken patches was sufficiently large to calculate a slope for the transition to 10,000 m^2.

Habitat	Area (m^2)					
	0.01–0.1	0.1–1	1–10	10–100	100–1,000	1000–10,000
Grassland	0.196	0.238	0.150	0.207	0.184	0.349
Woodland	0.081	0.173	0.242	0.193	0.437	0.439
Built	0.297	0.054	0.174	0.385	0.406	0.214
Bracken	0.064	0.058	0.094	0.274	0.423	n.a.
Heath	0.171	0.192	0.233	0.349	0.640	0.123
Fallow	0.244	0.141	0.119	0.256	0.225	0.320

intermediate scales (hectare to square kilometer) where whole new habitats are added as sample area is increased. At the largest spatial scales (10's to 1000's km^2), z is relatively small ($0.1 < z < 0.4$), reflecting the low turnover-with-distance that characterizes the British flora (*24*). These results raise important questions about the way that population dynamics creates spatial patterns (*30*), and about the way that spatial patterns (e.g., underlying heterogeneity in substrate) affect population dynamics. They also direct attention to the need to develop a more mechanistic understanding of coexistence at small scales (α diversity) and of distance-dependent turnover in species composition at landscape scales (γ diversity).

References and Notes

1. M. L. Rosenzweig, *Species Diversity in Space and Time* (Cambridge Univ. Press, Cambridge, 1995).
2. S. W. Pacala, in *Plant Ecology*, M. J. Crawley, Ed. (Blackwell Science, Oxford, 1997), pp. 532–555.
3. O. Arrhenius, *J. Ecol.* **9**, 95 (1921).
4. F. W. Preston, *Ecology* **43**, 185 (1962).
5. D. W. Goodall, *Biol. Rev.* **27**, 194 (1952).
6. R. A. Fisher, A. S. Corbet, C. B. Williams, *J. Anim. Ecol.* **12**, 42 (1943).
7. J. B. Plotkin *et al.*, *Proc. Natl. Acad. Sci. U.S.A.* **97**, 10850 (2000).
8. J. G. Skellam, *Biometrika* **39**, 346 (1952).
9. J. B. Plotkin *et al.*, *J. Theor. Biol.* **207**, 81 (2000).
10. E. C. Pielou, *An Introduction to Mathematical Ecology* (Wiley Interscience, New York, 1969).
11. M. W. Palmer, P. S. White, *Am. Nat.* **144**, 717 (1994).
12. J. Harte, S. McCarthy, K. Taylor, A. Kinzig, M. L. Fischer, *Oikos* **86**, 45 (1999).
13. W. E. Kunin, *Science* **281**, 1513 (1998).
14. E. F. Connor, E. D. McCoy, *Am. Nat.* **113**, 791 (1979).
15. R. M. May, in *Ecology and Evolution of Communities*, M. L. Cody, J. M. Diamond, Eds. (Harvard Univ. Press, Cambridge, MA, 1975), pp. 81–120.
16. G. Sugihara, *Am. Nat.* **116**, 770 (1980).
17. P. D. Kilburn, *Ecology* **47**, 831 (1966).
18. B. Hopkins, *J. Ecol.* **43**, 409 (1955).
19. R. Condit *et al.*, *J. Ecol.* **84**, 549 (1996).
20. G. Bell, *Am. Nat.* **155**, 606 (2000).
21. I. Hanski, M. Gyllenberg, *Science* **275**, 397 (1997).
22. J. Harte, A. Kinzig, J. Green, *Science* **284**, 334 (1999).
23. G. Sugihara, *Am. Nat.* **117**, 790 (1981).
24. M. J. Crawley, in *Plant Ecology*, M. J. Crawley, Ed. (Blackwell Science, Oxford, 1997), pp. 595–632.
25. G. C. Druce, *The Flora of Berkshire* (Clarendon, Oxford, 1897).
26. H. J. M. Bowen, *The Flora of Berkshire* (Holywell, Oxford, 1968).
27. C. Stace, *New Flora of the British Isles* (Cambridge Univ. Press, Cambridge, ed. 2, 1997).
28. We compared four statistical models for the Silwood data, using log-linear models corrected for overdispersion: a single slope; two piecewise slopes (using the left and right halves of the data); three piecewise slopes (using three, three, and six scales from small to large); and completely idiosyncratic slopes (10 different slopes). Each model was a significant improvement on the one before; deviance declined from 7583.0 to 5276.9 with 2 slopes, 5176.1 with 3 slopes, and 5143.2 with 10 slopes, as df declined from 1485 to 1483, 1480, then 1475.
29. We established 95% confidence intervals by taking 1000 random subsets of species richness data from each adjacent pair of scales, using a sample size that was half the size of the smallest of the two replicates. We used these smaller random subsets to compute 1000 values of z for each transition in scale. Tables 1 and 2 show the 2.5% and 97.5% percentiles for z.
30. B. M. Bolker, S. W. Pacala, *Am. Nat.* **153**, 575 (1999).
31. J. S. Rodwell, *British Plant Communities*, vols. 1 to 5 (Cambridge Univ. Press, Cambridge, 1991–1997).
32. A. Shmida, *Isr. J. Bot.* **33**, 41 (1984).
33. J.E.H. is supported by a Natural Environment Research Council studentship.

2 October 2000; accepted 20 November 2000

Lack of Replicative Senescence in Cultured Rat Oligodendrocyte Precursor Cells

Dean G. Tang,*† Yasuhito M. Tokumoto, James A. Apperly, Alison C. Lloyd, Martin C. Raff

Most mammalian somatic cells are thought to have a limited proliferative capacity because they permanently stop dividing after a finite number of divisions in culture, a state termed replicative cell senescence. Here we show that most oligodendrocyte precursor cells purified from postnatal rat optic nerve can proliferate indefinitely in serum-free culture if prevented from differentiating; various cell cycle–inhibitory proteins increase, but the cells do not stop dividing. The cells maintain high telomerase activity and p53- and Rb-dependent cell cycle checkpoint responses, and serum or genotoxic drugs induce them to acquire a senescence-like phenotype. Our findings suggest that some normal rodent precursor cells have an unlimited proliferative capacity if cultured in conditions that avoid both differentiation and the activation of checkpoint responses that arrest the cell cycle.

Classical replicative cell senescence in cultured human fibroblasts (*1*) is thought to depend on a cell-division counting mechanism, which is based on a progressive shortening and uncapping (*2*) of telomeres with prolonged proliferation, because it can be avoided by overexpression of the catalytic subunit of telomerase (*3–5*). Although proliferating rodent cells in culture tend to maintain telomerase activity and long telomeres (*3–5*), they also often permanently stop dividing and acquire a senescence-like phenotype. It has been suggested that this telomere-independent arrested state, which can also occur in human cells, may reflect a cell cycle checkpoint response to inappropriate culture conditions, rather than an intrinsic limitation imposed by a cell-division counting mechanism